applied sciences

MDPI

Article

A Simple Method to Estimate the In Situ Performance of Noise Barriers

Javier Redondo [1,*], Pau Gaja-Silvestre [1], Luis Godinho [2] and Paulo Amado-Mendes [2]

[1] Instituto de Investigación Para la Gestión Integrada de Zonas Costeras, Universitat Politècnica de València, C/Paranimf nº1, 46730 València, Spain; pgaja@silensacustica.com
[2] Department of Civil Engineering, University of Coimbra, ISISE, Rua Luís Reis Santos, 3030-788 Coimbra, Portugal; lgodinho@dec.uc.pt (L.G.); pamendes@dec.uc.pt (P.A.-M.)
* Correspondence: fredondo@fis.upv.es

Abstract: Noise barriers are usually classified attending to their intrinsic acoustic characteristics. This is standardized by the European Standards EN 1793, parts 2 and 6, in which a single parameter, DL_R or DL_{SI}, is defined in order to quantify the sound insulation performance of noise barriers. However, the final performance of a noise barrier, quantified by the so-called insertion loss, *IL* is not only dependent on the insulation provided by the noise barrier, but it is as well affected by geometrical aspects and the acoustic characteristics of the environment where these noise-reducing devices are placed. In this work, we explore the relationship between the insertion loss and the acoustic insulation by means of numerical methods. Moreover, the authors propose a simple way to predict the insertion loss from a purely acoustic numerical simulation in which this parameter is obtained for a completely rigid noise barrier, and knowing the noise barrier's sound reduction index, in one third octave bands.

Keywords: noise barriers; performance; numerical simulation

Citation: Redondo, J.; Gaja-Silvestre, P.; Godinho, L.; Amado-Mendes, P. A Simple Method to Estimate the In Situ Performance of Noise Barriers. *Appl. Sci.* **2022**, *12*, 7027. https://doi.org/10.3390/app12147027

Academic Editor: Michel Darmon

Received: 27 May 2022
Accepted: 8 July 2022
Published: 12 July 2022

1. Introduction

Traffic noise caused by vehicles is one of the most important and annoying sound problems all over the world and one of the main sources of environmental noise. This kind of noise has worsened significantly in recent years, mainly due to the increase in population mobility and high traffic density on the roads. In general, this sound pollution level depends on the noise generated by the vehicle engines and their speed, but also on the road surface and on the type of pavement of the infrastructure.

The most commonly used solution to mitigate the effects of road traffic noise during transmission is the placement of noise barriers, also known as noise reduction devices (DRRs) in the European standards. Classical noise barriers, usually formed by continuous flat walls, are located between the noise source (transport infrastructure) and the receiver (adjacent dwellings or other sensitive receivers).

Noise barriers are commonly classified attending to their acoustic insulation [1,2], apart from sound absorption that plays a secondary role. There are two standards that describe different parameters to quantify the insulating performance of noise barriers. The first one is the so-called single-number rating of airborne sound insulation, DL_R, defined as a weighted average of the sound reduction index, R_i, for each one third octave band, that considers both the sound source spectra (traffic noise) and the listener sensitivity (in dBA). The sub index *I* is the index of each one third octave band. Namely, it is expressed by:

$$DL_R = -10log\left|\frac{\sum_{i=1}^{18} 10^{0.1\ L_i} 10^{-0.1\ R_i}}{\sum_{i=1}^{18} 10^{0.1\ L_i}}\right| \text{ dBA} \quad (1)$$

where L_i are the values of the normalized traffic noise spectrum, given by the standard EN 1793-3 [3], and R_i are the one third octave band values of the sound reduction index of the noise barrier, described in standard EN 10140-2 [4].

Following the recommendations of this measurement standard, it is valid only in the case of reverberant conditions, i.e., the sound field impinging the noise barrier is diffuse. Nevertheless, it is still used in some countries due to the problems associated with in-situ measurements, i.e., ambient noise, complicated signal processing, need for microphonic arrays, etc.

A second method to quantify the sound insulation provided by the noise screen is described in the standard [2]. This standard describes an in-situ test method in which measurements are carried close to the barrier. An appropriate temporary windowing (Adrienne temporal windows) is used to avoid the problems associated with edge diffraction. The single-number quantity to estimate the overall sound insulation defined in that standard is the following:

$$DL_{SI} = -10 \log \left[\frac{\sum_{i=m}^{18} 10^{0.1L_i} 10^{-0.1SI_i}}{\sum_{i=m}^{18} 10^{0.1L_i}} \right] \text{dBA} \quad (2)$$

where L_i are the values of the normalized traffic noise spectrum, given by the standard EN 1793-3 [3] and SI_i are the one third octave band values of the sound insulation index derived from in situ measurements. One of the problems associated with this standard is the existence of a limiting frequency below which measurements are unreliable due to the limited length of the Adriane window used to avoid edge diffraction. The height of the barrier determines the value of this cut-off frequency.

In any case, the final performance of the screen is not only dependent on the acoustic insulation but also on the particular geometry (shape of the ground, position of the sound source and listeners, and shape of the noise barrier) and other aspects, such as the ground acoustic absorption. The final performance is quantified by a parameter known as Insertion Loss [5] (IL_i, the subindex i stands for the particular one third octave band considered) which is nothing more than the difference between the sound pressure levels for the situation before installing (without) the screen and after installing (with) the screen, namely:

$$IL_i = 10 \log \left(\frac{p_{i\ (without)}}{p_{i\ (with)}} \right)^2 \quad (3)$$

To allow the comparison between parameters, let us define a single parameter that quantifies the effect of the screen encompassing the whole frequency range of interest by means of a weighting, analogous to that already indicated when defining DL_R and DL_{SI}, i.e.,:

$$DL_{IL} = -10 \log \left| \frac{\sum_{i=1}^{18} 10^{0.1\ L_i} 10^{-0.1\ IL_i}}{\sum_{i=1}^{18} 10^{0.1\ L_i}} \right| \text{dBA} \quad (4)$$

where L_i are the values of the normalized traffic noise spectrum, given by the standard EN 1793-3 [3], and IL_{i} is the insertion loss for the i-th one third octave band.

Many simple formulae and charts to estimate the insertion loss of semi-infinite noise barriers can be found in the literature. The first attempt was published by Redfearn [6], while Maekawa [7] presented the best-known work. Maekawa [7] performed an exhaustive experimental investigation validating his proposal, based on a single parameter, the Fresnel number. Subsequently, other authors proposed different approaches to the problem. Without being exhaustive, it is worth mentioning the works of Rathe [8] and Kurze and Anderson [9,10]. Another simple formula, in good agreement with Maekawa [7] data, was proposed by Tatge [11] that has been included in the ISO 9613-2 [12].

Predictions obtained by these formulae and charts can deviate largely from experimental data in some cases. To solve this problem, numerical methods can be used to estimate the performance of noise barriers. Numerical methods such as the Finite Element Method (FEM), the Boundary Element Method (BEM), the Pseudo Spectral Time Domain (PSTD)

method and the Finite Difference Time Domain (FDTD) method have been applied to the study of noise barriers. For convenience the authors have used the later method in this work. Several papers have demonstrated the suitability of this method for the study of sound propagation in the presence of acoustic screens [13–16].

In any case, both approximate formulas and numerical simulations usually assume a high insulation, so that sound transmission through the barrier is not taken into account. For example, in [12] it is assumed that the surface density is at least 10 kg/m^2, which should ensure an overall insulation above 25 dBA.

In this work, a simple model is proposed to obtain the insertion loss value in the case that the insulation of the material with which the screen is constructed allows significant sound transmission thorough the barrier. The remaining part of the paper is organized as follows: first, Section 2 concerns the proposal of the simple model to estimate the insertion loss of a noise barrier; in Section 3 the numerical method used to verify the proposed model is explained; Section 4 is devoted to the comparison between the proposed model and the numerical simulations; finally, the conclusions of the work are presented in Section 5.

2. Proposed Model

In this section a simple method will be described to obtain the insertion loss provided by a noise barrier without requiring specific measurements or a complete vibroacoustic simulation of the behaviour of the acoustic screen.

Consider the simple scenario of a noise barrier illustrated in Figure 1. The effect of the acoustic screen can be understood through the Huygens–Fresnel–Kirchhoff principle. Energy from the plane wave impinging the noise barrier can travel through the screen or can pass over it, and both contributions will arrive to each measurement position. If ε is the portion of the energy that arrives to a particular measurement position propagating above the acoustic screen, the portion that travels through the screen will be $(1-\varepsilon)\tau$, τ being the corresponding sound transmission coefficient. Then, if no reflections are considered, the frequency-dependent Insertion Loss can be written as:

$$IL_i = -10\log[(1-\varepsilon_i)\tau_i + \varepsilon_i] \tag{5}$$

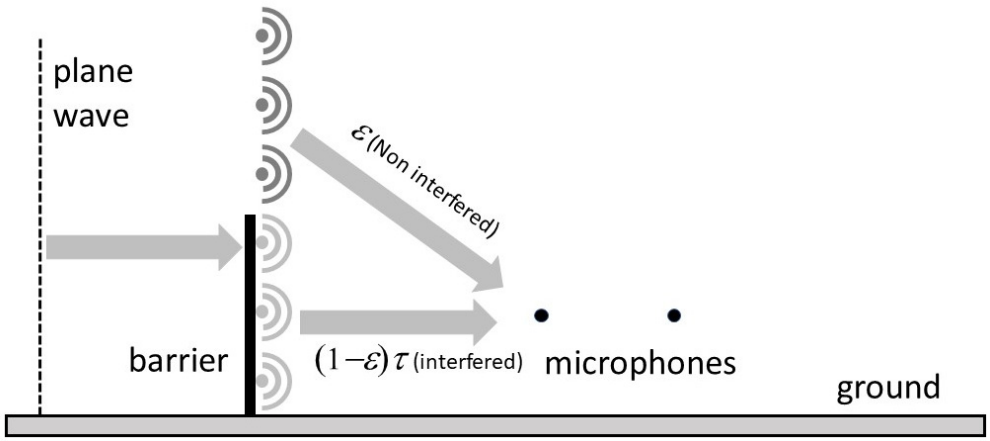

Figure 1. Schematic representation of a noise barrier, showing the application of the Huygens–Fresnel–Kirchhoff principle.

The frequency dependent transmission factor, τ_i, is related to the sound reduction index by the expression:

$$R_i = 10\log\left(\frac{1}{\tau_i}\right) \tag{6}$$

Notice that incoherence is assumed between the sound not interfered by the acoustic screen and the one that goes through it. Nevertheless, the third octave averaging performed in all of the aforementioned standards reduces the effect of coherent terms in the sum of the two contributions.

The portion of energy not interfered by the noise barrier, ε, can be obtained from the numerical simulation of the particular geometry under study, forcing the screen to be completely rigid and reflective ($\tau = 0$), which is the easiest case to be simulated, without taking into account the vibrational problem inside the noise barrier. In that case, Equation (5) is written as

$$IL_{i\ rigid} = -10\log[\varepsilon_i] \tag{7}$$

In other words,

$$\varepsilon_i = 10^{-IL_i\ rigid/10} \tag{8}$$

As a result, the final performance of an acoustic screen can be obtained by knowing the reduction index, R, commonly provided by the manufacturer, and the particular value of ε that, as commented before, can be obtained from the simulation of the limiting case in which the noise barrier is completely stiff and reflective. In other words, there is no need to perform a vibroacoustic simulation of the acoustic screen that takes into account the transmission of sound through the material or materials it is made of. Notice that, for that particular case, ε can be easily obtained with common numerical methods used in acoustics (such as FEM, FDTD, BEM or MFS) through simple 2D numerical simulations in vertical plane, given that the partial sound insulation of the acoustic screen is not needed.

3. Fdtd Simulations

As commented above, the FDTD method has been chosen in this work. A 2D acoustic simulation scheme using FDTD has been developed, schematically illustrated in Figure 2, hereafter referred to as XZ simulation model. Although further details of the numerical technique can be found in the literature, for completeness, the fundamental concepts are given next.

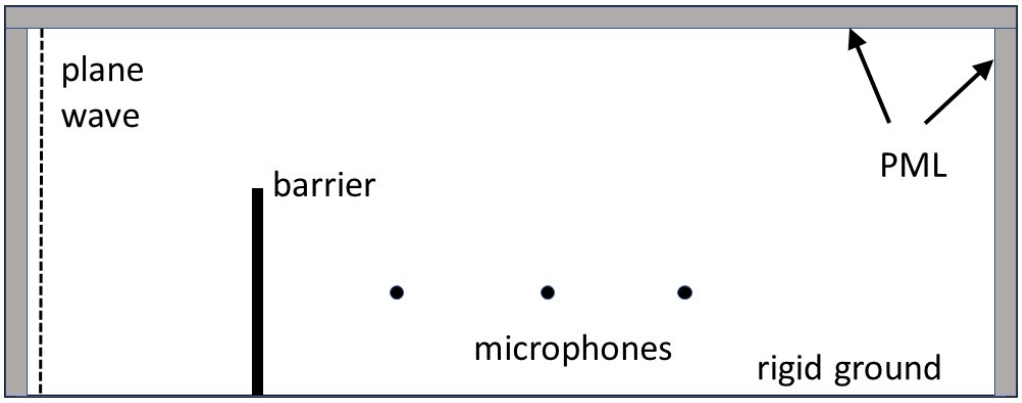

Figure 2. Schematic representation of the FDTD model, used in the XZ simulation, including indication of the considered boundary conditions.

The acoustic FDTD model with no sound sources is governed by the equations for conservation of momentum and continuity. In a homogeneous medium with no losses, these can be written as:

$$\frac{\partial p}{\partial t} + k\vec{\nabla}\cdot\vec{u} = 0 \tag{9a}$$

$$\vec{\nabla} p + \rho_0 \frac{\partial \vec{u}}{\partial t} = 0 \tag{9b}$$

where p is the pressure field, $\vec{u} = (u_x, u_z)$ is the vector particle velocity field, ρ_0 is the mass density of the medium and $k = \rho_0 c^2$ is the compressibility of the medium. The partial derivatives (space and time) of pressure and particle velocity can be approximated by well-known central finite difference schemes; for instance, in the case of the sound pressure derivative with respect to x, this approximation can be given as

$$\left.\frac{\partial p}{\partial x}\right|_{x=x_0} \approx \frac{p\left(x_0 + \frac{\Delta x}{2}\right) - p\left(x_0 - \frac{\Delta x}{2}\right)}{\Delta x} \tag{10}$$

with Δx being the spatial interval between two consecutive points in the x direction. In the case of 2D problems, three grids must be defined, namely one grid for pressure and one grid for each of the particle velocity components (x and z). To minimize the significance of higher order terms, those grids are 'staggered', which means that, for example, the meshes for the x and z components of the particle velocity are shifted a distance of $\Delta x/2$ and $\Delta z/2$ with respect to the pressure mesh; the same principle is applied to the time discretization, in which the particle velocity meshes are shifted $\Delta t/2$ in time with respect to the pressure mesh. A set of update equations can then be obtained to compute the values of pressure and particle velocity after repetition for a given number of time steps. A detailed description of all relevant equations is given in [17].

In order to avoid unwanted numerical reflections in the considered rectangular numerical calculation domain, a Perfectly Matched Layer (PML) [18] is located at three of the four numerical domain boundaries, depicted in Figure 2. Bear in mind that the sound can be reflected on the ground, corresponding to the lower horizontal boundary. Without loss of generality, in this work, a completely rigid floor will be considered, in other words, total reflection is assumed on the ground surface. With these boundary conditions, the numerical domain is excited by a plane wave travelling from left to right. The acoustic measurements have been numerically recorded at the microphones, located at the shadow area of a classical noise barrier. This FDTD model assumes that all the propagation domain is air, except the ground surface and the acoustic barrier that are completely stiff and reflective.

The described FDTD simulation model can be easily adapted to verify the accuracy of the simplified model discussed above. The modification consists of adding the possibility of simulating the transmission of sound through the noise barrier without the simulation of the full vibroacoustic problem. Figure 3 includes a schematic representation of this modification. The signal obtained at the pressure points (labelled as "recorded" in the figure), on the left side of the acoustic screen, is taken and re-injected at the x-velocity points (labelled as "injected" in the figure) that define the screen contour on the right side of the screen once multiplied by a transmission factor (τ). There are two aspects to take into account. As the recorded signal corresponds to pressure points and it is being re-injected at velocity points, the signal must be divided by the specific acoustic impedance of the air. In addition, at the pressure points, not only the incident wave but also the reflected wave by the screen are recorded. If the screen is considered as infinitely rigid and reflective, i.e., zero sound absorption is assumed, both incident and reflected waves are of equal level and also in phase, so that the pressure at the "recorded" points is exactly twice that of the incident pressure. Taking this into account, the signal is divided by 2. If the transmission factor is considered to be frequency dependent, a pre-filter should be added before re-injecting the signal. For simplicity, only the results for non-frequency dependent transmission factors are shown in this paper. This model is hereafter referred to as "modified FDT".

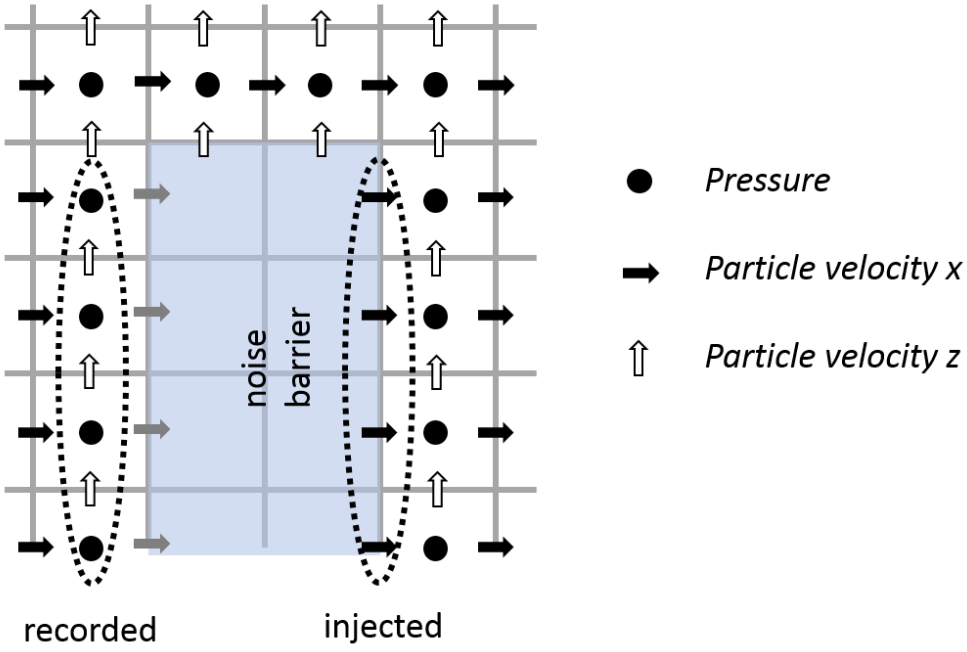

Figure 3. Schematic representation of the locations of the particle velocities and acoustic pressures grid nodes near the noise barrier in the modified FDTD simulation model, for the simulation of sound transmission through the noise barrier.

4. Model Validation

In this section, the results obtained in the simulations using the FDTD method are reported and compared with the simple model proposed in Section 2. It will be shown that this model provides an excellent approximation to the noise shielding produced by an acoustic screen. In the following, the results presented are averaged over one third of an octave frequency bands. For clarity, a subscript i is added (representing the i-th band) to indicate that the magnitudes are averaged in this way.

4.1. Application to Traditional Noise Barriers

Initially, the application of the simple model to traditional barriers is considered. For brevity, only the results for a 3 m-high acoustic screen, with the measurement microphones placed at a height of 1.5 m and a distance to the screen of 4 m, will be shown. To simulate the 3D conditions, the results obtained for larger distances are averaged, as described by [19,20], in order to correctly simulate an incoherent line source based on several two-dimensional coherent line source simulations.

The results of the numerical simulations carried out are illustrated in Figure 4, for the case of the model shown in Figure 2 (conventional noise barrier). For clarity, Figure 4 includes only four representative values of the noise barrier's sound reduction index, R (6, 12, 18 dB and the perfectly rigid and reflective case, R = ∞), with constant values of R assigned to all one third octave bands.

In Figure 4, the results of the IL index as a function of the frequency, for different values of noise reduction, R, are shown, considering for each case the same value of R_i for all the analysed frequencies. The first thing that can be seen is the good agreement between the values obtained by means of the "modified FDTD" model and by the simple model proposed in this paper (Equation (5)). The agreement is not so good in the low frequency range where the assumption of incoherence is less likely to be adequate. However, the most interesting conclusion is the smaller difference values of insertion loss, IL, when compared with the corresponding R values, for the less insulating noise barriers. This result is logical, taking into account that the parameter IL not only considers the transmitted wave but also the diffracted wave, which considerably reduces the performance of the noise barrier, mainly for the higher insulation ones. Moreover, if

an infinite value of R is considered, the IL index is maximized, reaching a value around 20 dB for higher frequencies. This means that, no matter how much the acoustic insulation of a noise barrier is increased (thus decreasing the transmission through them) their final performance, given by IL, reaches a maximum and saturates.

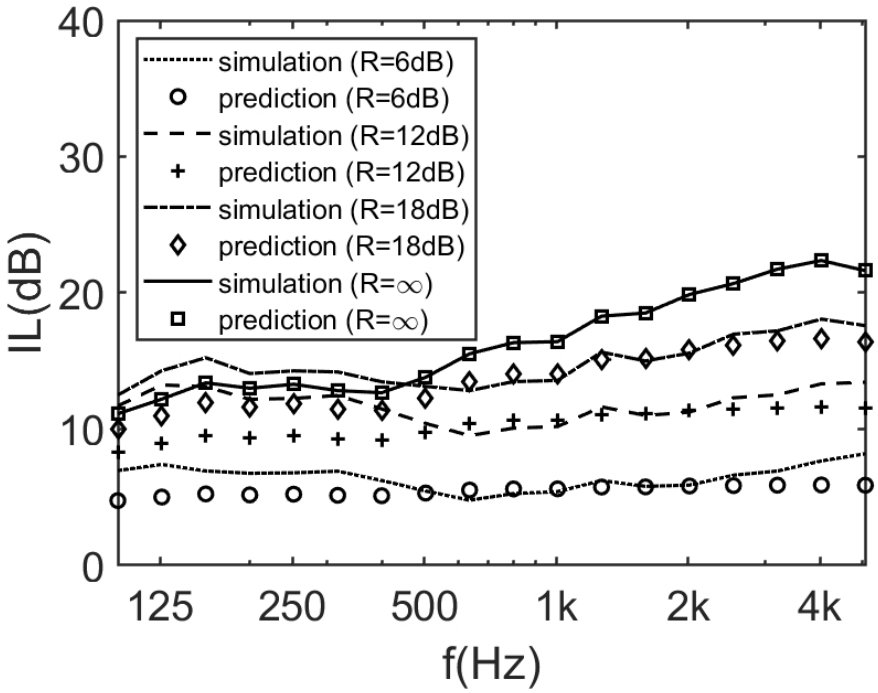

Figure 4. Values of IL index, predicted using the proposed simple model (Equation (5)) and simulated with the "modified FDTD" model, as a function of the frequency, for different values of noise reduction, R.

This trend is more clearly seen in Figure 5, where the relationship between the global IL (DL_{IL}) and DL_R indexes is represented. In this figure, the dashed line represents the global insulation of the noise barrier, given by DL_R index (when diffraction at the top of the noise barrier is not taken into account). The continuous line indicates the variation in the global IL index with the increase in the acoustic insulation (DL_R). Again, one can see that the saturation in the global acoustic performance of the noise barrier is around 15 dBA, although the DL_R value still increases. That means that the final performance of the noise barrier should be estimated with the global IL index and not the acoustic insulation (DL_R). For better comparison of the results, the numerical values and the absolute differences are provided in Table 1.

Table 1. Comparison of the values of global IL (DL_{IL}) obtained from the FDTD numerical simulation and the simple model proposed in this work (Equation (5)) for different values of the airborne sound insulation (DL_R). The absolute differences are always below a JND (1 dBA).

DL_R	DL_{IL} (dBA) FDTD Simulation	DL_{IL} (dBA) Simplified Proposed Model (Equation (5))	Absolute Difference (dBA)
6.0	5.9	5.6	0.3
12.0	11.0	10.5	0.5
18.0	14.3	13.8	0.6
24.0	15.7	15.2	0.4
30.0	16.0	15.7	0.3
35.0	16.0	15.8	0.2

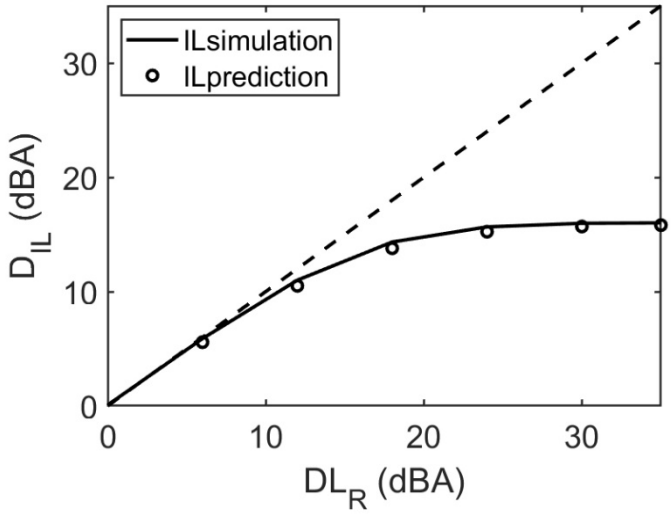

Figure 5. Relationship between global IL (DL_{IL}) and DL_R indexes. Black dashed line indicates the ideal behaviour of a noise barrier if diffraction at the upper edge is not considered (infinite height). Continuous line represents the variation of DL_{IL} index as a function of DL_R index obtained by the numerical FDTD simulation. Dots represent the global IL index obtained by the simple method proposed in this work (Equation (5)).

4.2. Application to Noise Barriers Based on Sonic Crystals

In the last few years, several authors have demonstrated the applicability of sonic crystals as noise barriers with the additional advantage of being almost transparent to wind and water [21]. Figure 6 illustrates a prototype of this kind of noise reduction devices. Sonic crystals are defined as heterogeneous materials formed by periodic arrangements of acoustic scatterers, commonly cylindrical elements, embedded in air and organized in a regular lattice distribution with a minimum distance between the centres of the scatterers, called lattice constant. These open acoustic screens present a new wave control mechanism due to the arrangement of the scatterers, which provides the appearance of bandgaps, defined as frequency ranges where the propagation of waves is forbidden or blocked. As a result, these structures can be effectively used as noise barriers providing significant attenuation in the bandgaps' frequency range.

In order to validate the proposed model for the case of noise barriers based on sonic crystals, the transmission coefficients, obtained from a classical 2D numerical simulation of the sound propagation through the sonic crystal using the FDTD numerical model (in the plane XY, see Figure 7), have been used (in the plane XY, see Figure 7). These results have been combined with Equation (5), using the non-interfered values of ε_i obtained from the XZ numerical simulation commented in the previous section, for the case of infinite acoustic insulation. To validate the proposed model results, they have been compared with the ones obtained from a full 3D numerical simulation model [22] (see Figure 7 with a schematic representation of a sector of the 3D noise barrier). These results are summarized and can be compared in Figure 8. Again, for the sake of clarity, only three representative values of the diameter of the cylinders forming the sonic crystal barrier are used. The presented cases are the following: scatterers diameter (d) equal to 50%, 75% and 90% of the lattice constant (lc). The lattice constant (lc = 0.17 m) has been chosen to make the first band gap appear around 1 kHz, which is the more relevant band for traffic noise according to [4].

From the results illustrated in Figure 8, it can be seen that the agreement is very good for medium and high frequencies. Nevertheless, in the range of low frequencies, as commented before, the effects of coherence between the interfered and non-interfered contributions worsen the results being compared. However, the small deviations at low frequencies are negligible when the overall insulation indices are being computed for the noise barriers.

Figure 6. Prototype of a noise barrier based on sonic crystals.

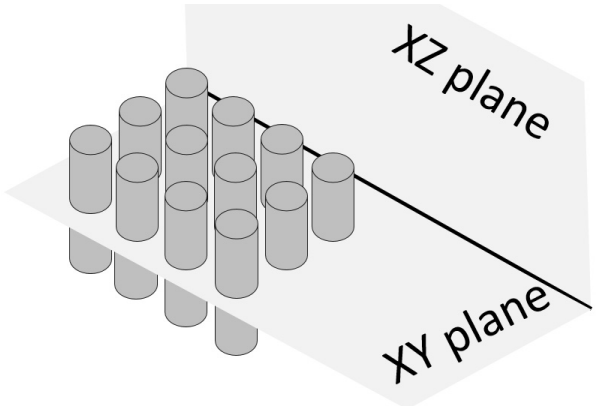

Figure 7. Schematic view of the simulation planes.

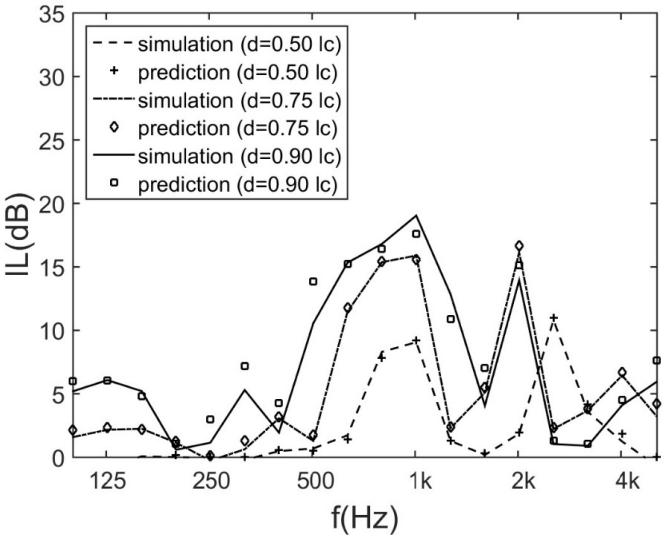

Figure 8. Values of IL index of sonic crystals noise barriers with different scatterer diameters. The lines correspond to 3D numerical simulations [22]. Lines with marks correspond to predictions using the model proposed in this paper (Equation (5)). Three values of the scatterers' diameter (d) are plotted relative to the lattice constant (lc). (d = 50%, 70% and 90% of the lattice constant).

4.3. Comparison with "Overlapping Model"

Concerning noise barriers based on sonic crystals, there are several works where methods of combining different numerical simulations have been proposed in order to avoid the need to perform 3D numerical simulations to obtain the noise barriers' insertion loss curve [23,24]. In these methods, called by the authors as "overlapping models", the 3D problem is divided into two 2D schemes, namely in the XY and XZ planes, obtaining the IL values of the 3D case as:

$$IL(f) = 10\log\left(\left|\frac{p_{without}}{p_{withXY} + p_{withXz}}\right|\right)^2 \tag{11}$$

where $p_{without}$ is the sound pressure without the acoustic screen, p_{withXY} is the sound pressure with the acoustic screen in the XY plane simulation and p_{withXZ} is the sound pressure with the acoustic screen in the XZ plane simulation. In the aforementioned works, the authors distinguish between the contributions of incident sound and scattered sound. Notice that the summation in the denominator is complex, i.e., it takes into account the phase changes in each of the 2D orthogonal simulations.

It should be noted that this approximation is not valid in the limiting cases where the barrier does not provide any shielding, since in that case $p_{without} = p_{withXY} = p_{withXZ}$, resulting in a value of -6 dB when it should be 0 dB. It is also assumed that the acoustic path between sources and receivers is identical in the two 2D orthogonal simulations that are combined to obtain the full model.

Figure 9 illustrates the results for the two approximate models together with the exact solution obtained in a 3D simulation. In general, an excellent agreement is observed between the results of the model proposed in this work and the 3D simulations. This is not the case for the model of Castiñeira et al. [23,24]. As already indicated, this model also combines two numerical simulations, but the underlying philosophy is quite different.

If insertion loss concept is translated into transmission coefficients it may be easier to compare the "overlapping method" proposed by Castiñeira et al. [23,24] and the simple method proposed in this paper (Equation (5)). A global transmission coefficient, τ_G, can be defined as follows,

$$IL = 10\log\left(\frac{1}{\tau_G}\right) \tag{12}$$

In other words,

$$\tau_G = 10^{-IL/10} \tag{13}$$

In the case of the "overlapping method" proposed by Castiñeira et al. [23,24], this coefficient is calculated as:

$$\tau_{G\,OM} = \left(\left|\frac{p_{withXY} + p_{withXZ}}{p_{without}}\right|\right)^2 \tag{14}$$

where OM stands for the "overlapping method" proposed by Castiñeira et al. [23,24]. Assuming incoherence between the two 2D models, it can be written as follows,

$$\tau_{G\,OM} = \tau_{XY} + \tau_{XZ} \tag{15}$$

This can lead to values of the transmission coefficient outside the physically meaningful limits, above 1. Moreover, taking into account the phase of the coefficients in Equation (12) could lead to a value of 4 in the case of a completely transparent screen, when it should be 1.

For a better comparison between the two methods, we can restate the model proposed in this work in terms of the transmission coefficients obtained in the XY and XZ simulations.

So, in Equation (5), ε will be substituted by τ_{XZ} and τ will be substituted by τ_{XY}. Therefore, the global transmission coefficient can be expressed as:

$$\tau_G = (1 - \tau_{XZ})\tau_{XY} + \tau_{XZ} = 1 - (1 - \tau_{XY})(1 - \tau_{XZ}) = \tau_{XY} + \tau_{XZ} - \tau_{XY}\,\tau_{XZ} \quad (16)$$

This transmission coefficient is bounded between 0 and 1, as opposed to the "overlapping model". This is especially noticeable for high values of the transmission coefficients, which for example appear in the low frequency range for small values of the diameter of the scatterers (top plots in Figure 9).

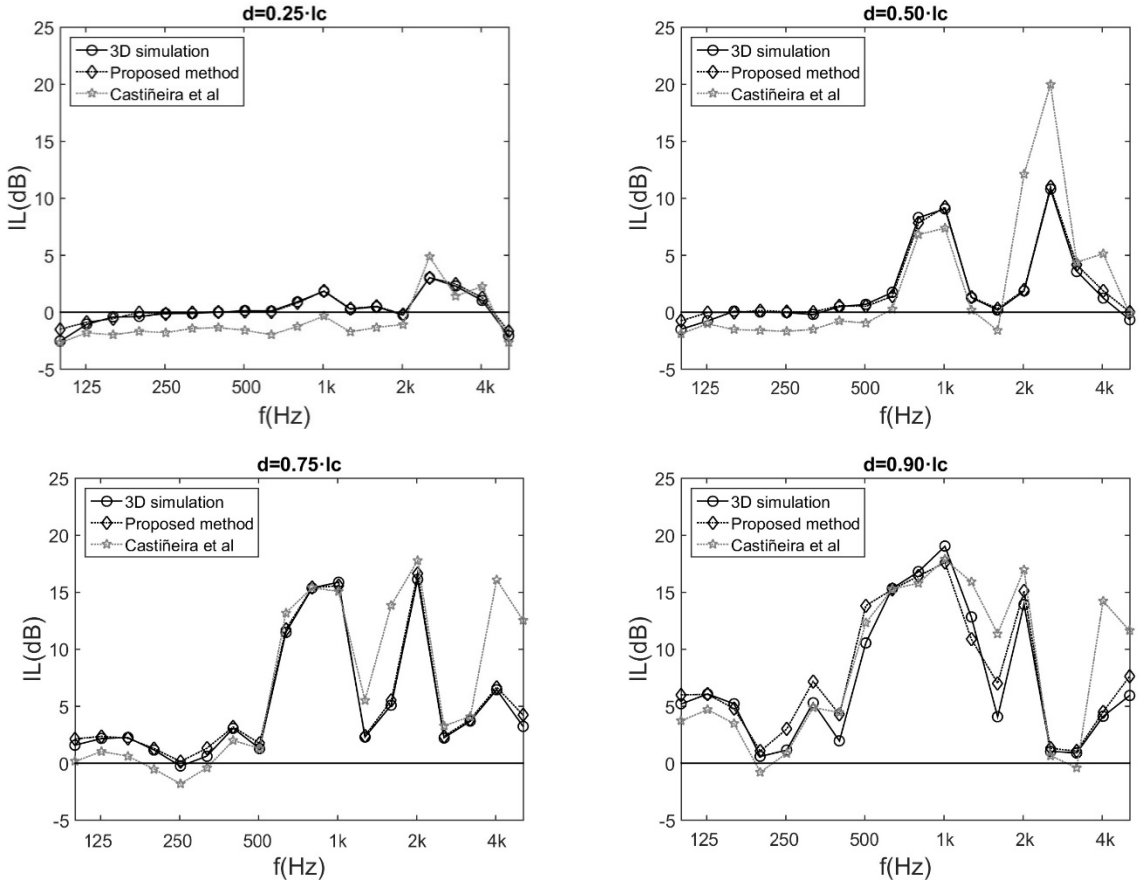

Figure 9. Comparison of the values of IL provided by the proposed method (Equation (5)) and the "overlapping method" proposed by Castiñeira et al. [23,24]. Different relations between the diameter of the scatterers and the lattice constant are illustrated. Top left, 25%; top right, 50%; bottom left, 75%; and bottom right, 90%. (Lines with circular markers: 3D numerical simulation; Lines with rhombus markers: proposed model (Equation (5)); Lines with star markers: "overlapping method" by Castiñeira et al. [23,24]).

Finally, it should be noted that the model proposed and validated in this work is comparable to the calculation of the insulation provided by composite heterogeneous walls. The simplest way to predict the behaviour of a wall composed of two materials is a weighted average of the transmission coefficients of each material, being the weights of each component calculated as the surface area of each material divided by the total surface area. In the case of the model proposed in this work, the effective surface area of each of the components is calculated in the case where one of the materials has a transmission coefficient of unity (corresponding to the portion of sound travelling over the noise barrier) and the other material (the noise barrier itself) has a transmission coefficient of 0.

5. Conclusions

The acoustic performance of traffic noise barriers, regarding sound insulation, is normally evaluated by standardized parameters, such as the single-number rating of airborne sound insulation, DL_R, or the single-number sound insulation rating, DL_{SI}. However, the final performance of these noise reduction devices, being also dependent on in situ specificities, is more often characterized by the Insertion Loss frequency-dependent curve, IL_i, or the corresponding weighted single-number, DL_{IL}, which has been estimated by different authors. In this work, based on the Huygens–Fresnel–Kirchhoff principle, a simplified model is proposed to obtain the Insertion Loss provided by a noise barrier, assuming that the noise barrier's sound reduction index is known and only a numerical acoustic simulation, with a completely rigid noise barrier, has to be performed. This simplified model is herein verified by comparison with a FDTD numerical simulation method, applied to both traditional and sonic crystal-based noise barriers. Then, the relationship between the two parameters used in the quantification of the acoustic performance of noise barriers, namely, the Insertion Loss (IL) and the airborne sound insulation (DL_R), was explored. The good agreement between the values obtained by the FDTD model and by the simple model proposed in this paper was shown, but was also interestingly demonstrated that, no matter how much the acoustic insulation of a noise barrier is increased, its final performance, given by the Insertion Loss parameter, reaches a maximum and saturates, being controlled by the diffraction at the top of the noise barrier. In the case of noise barriers based on sonic crystals, very good Insertion Loss results have been observed for different filling factors of the crystal distribution, in comparison to 3D simulations, mainly in the medium and high frequencies ranges. These conclusions have been corroborated with "overlapping models" [23,24], and the similarity of the simple proposed model with the evaluation of the insulation achieved by composite heterogeneous panels has been highlighted, making use of the transmission coefficient of the noise barrier.

Author Contributions: Conceptualization, J.R.; methodology, P.G.-S., L.G. and P.A.-M.; software, J.R.; validation, L.G. and P.A.-M.; formal analysis, P.G.-S.; data curation, P.G.-S.; writing—original draft preparation, J.R.; writing—review and editing, L.G. and P.A.-M.; All authors have read and agreed to the published version of the manuscript.

Funding: This work was supported in part by the grant "PID2019-109175GB-C22" funded by MCIN/AEI/10.13039/501100011033. This work was developed within the scope of the POCI-01-0247-FEDER-033990 (iNBRail) co-funded by FEDER, through the Operational Programme for Competitiveness and Internationalization (POCI), and POCI-01-0247-FEDER-033691 (HLS—Hybrid Log Shield) Projects, funded by FEDER funds through COMPETE 2020. This work was also funded by Base Funding —UIDB/04029/2020—of ISISE (Institute for Sustainability and Innovation in Structural Engineering) funded by national funds through the FCT/MCTES (PIDDAC).

Institutional Review Board Statement: Not applicable.

Informed Consent Statement: Not applicable.

Data Availability Statement: Not applicable.

Conflicts of Interest: The authors declare no conflict of interest.

References

1. *EN 1793-2*; Road Traffic Noise Reducing Devices—Test Method for Determining the Acoustic Performance—Part 2: Intrinsic Characteristics of Airborne Sound Insulation under Diffuse Sound Field Conditions. CEN: Brussels, Belgium, 2012.
2. *EN 1793-6*; Road Traffic Noise Reducing Devices—Test Method for Determining the Acoustic Performance—Part 6: Intrinsic Characteristics—In Situ Values of Airborne Sound Insulation under Direct Sound Field Conditions. CEN: Brussels, Belgium, 2012.
3. *EN 1793-3*; Road Traffic Noise Reducing Devices—Test Method for Determining the Acoustic Performance—Part 3: Normalized Traffic Noise Spectrum. CEN: Brussels, Belgium, 2012.
4. *ISO 10140-2*; Acoustics—Laboratory Measurement of Sound Insulation of Building Elements—Part 2: Measurement of Airborne Sound Insulation. International Organization for Standardization (ISO): Geneva, Switzerland, 2021.
5. *ISO 10847*; Acoustics—In-Situ Determination of Insertion Loss of Outdoor Noise Barriers of All Types. International Organization for Standardization (ISO): Geneva, Switzerland, 1997.

6. Redfearn, S. XX. Some acoustical source-observer problems. *Lond. Edinb. Dublin Philos. Mag. J. Sci.* **1940**, *30*, 223–236. [CrossRef]
7. Maekawa, Z. Noise reduction by screens. *Appl. Acoust.* **1968**, *1*, 157–173. [CrossRef]
8. Rathe, E. Note on two common problems of sound propagation. *J. Sound Vib.* **1969**, *10*, 472–479. [CrossRef]
9. Kurze, U.; Anderson, G. Sound attenuation by barriers. *Appl. Acoust.* **1971**, *4*, 35–53. [CrossRef]
10. Kurze, U.J. Noise reduction by barriers. *J. Acoust. Soc. Am.* **1974**, *55*, 504–518. [CrossRef]
11. Tatge, R. Barrier-wall attenuation with a finite-sized source. *J. Acoust. Soc. Am.* **1973**, *53*, 1317–1319. [CrossRef]
12. *ISO 9613-2*; Acoustics—Attenuation of Sound during Propagation Outdoors—Part 2: General Method of Calculation. International Organization for Standardization (ISO): Geneva, Switzerland, 1996.
13. Sakamoto, S.; Seimiya, T.; Tachibana, H. Visualization of sound reflection and diffraction using finite difference time domain method. *Acoust. Sci. Technol.* **2002**, *23*, 34–39. [CrossRef]
14. Yokota, T.; Hirao, Y.; Yamamoto, K. Efficient calculation on outdoor sound propagation by FDTD and PE methods. *Acoust. Sci. Technol.* **2006**, *27*, 177–179. [CrossRef]
15. Van Renterghem, T.; Botteldooren, D. Numerical simulation of the effect of trees on downwind noise barrier performance. *Acta Acust. United Acust.* **2003**, *89*, 764–778.
16. Heimann, D. On the efficiency of noise barriers near sloped terrain—A numerical study. *Acta Acust. United Acust.* **2010**, *96*, 1003–1011. [CrossRef]
17. Redondo, J.; Picó, R.; Roig, B.; Avis, M.R. Time domain simulation of sound diffusers using finite-difference schemes. *Acta Acust. United Acust.* **2007**, *93*, 611–622.
18. Yuan, X.; Borup, D.; Wiskin, J.W.; Berggren, M.; Eidens, R.; Johnson, S.A. Formulation and validation of Berenger's PML absorbing boundary for the FDTD simulation of acoustic scattering. *IEEE Trans. Ultrason. Ferroelectr. Freq. Control* **1997**, *44*, 816–822. [CrossRef]
19. Van Renterghem, T.; Salomons, E.; Botteldooren, D. Parameter study of sound propagation between city canyons with coupled FDTD-PE model. *Appl. Acoust.* **2006**, *67*, 487–510. [CrossRef]
20. Defrance, J.; Salomons, E.; Noordhoek, I.; Heimann, D.; Plovsing, B.; Watts, G.; Jonasson, H.; Zhang, X.; Premat, E.; Schmich, I.; et al. Outdoor sound propagation reference model developed in the European Harmonoise project. *Acta Acust. United Acust.* **2007**, *93*, 213–227.
21. Sánchez-Pérez, J.V.; Caballero, D.; Martinez-Sala, R.; Rubio, C.; Sanchez-Dehesa, J.; Meseguer, F.; Llinares, J.; Galvez, F. Sound Attenuation by a Two-Dimensional Array of Rigid Cylinders. *Phys. Rev. Lett.* **1998**, *80*, 5325–5328. [CrossRef]
22. Godinho, L.; Redondo, J.; Amado-Mendes, P. The method of fundamental solutions for the analysis of infinite 3D sonic crystals. *Eng. Anal. Bound. Elem.* **2019**, *98*, 172–183. [CrossRef]
23. Castiñeira-Ibáñez, S.; Rubio, C.; Sánchez-Pérez, J.V. Acoustic wave diffraction at the upper edge of a two-dimensional periodic array of finite rigid cylinders. A comprehensive design model of periodicity-based devices. *Europhys. Lett.* **2013**, *101*, 64002. [CrossRef]
24. Castiñeira-Ibáñez, S.; Rubio, C.; Sánchez-Pérez, J.V. Environmental noise control during its transmission phase to protect buildings. Design model for acoustic barriers based on arrays of isolated scatterers. *Build. Environ.* **2015**, *93*, 179–185. [CrossRef]